MDPI

Article

A Revival of Molecular Surface Electrostatic Potential Statistical Quantities: Ionic Solids and Liquids

Jane S. Murray [1],* , Kevin E. Riley [2] and Tore Brinck [3]

1   Department of Chemistry, University of New Orleans, New Orleans, LA 70148, USA
2   Department of Chemistry and Biology, Xavier University of New Orleans, New Orleans, LA 70125, USA; kriley3@xula.edu
3   Department of Chemistry, KTH Royal Institute of Technology, SE-100 44 Stockholm, Sweden; tore@kth.se
*   Correspondence: jane.s.murray@gmail.com

Abstract: In this paper, we focus on surface electrostatic potentials and a variety of statistically derived quantities defined in terms of the surface potentials. These have been shown earlier to be meaningful in describing features of these potentials and have been utilized to understand the interactive tendencies of molecules in condensed phases. Our current emphasis is on ionic salts and liquids instead of neutral molecules. Earlier work on ionic salts has been reviewed. Presently, our results are for a variety of singly charged cations and anions that can combine to form ionic solids or liquids. Our approach is computational, using the density functional B3PW91/6-31G(d,p) procedure for all calculations. We find consistently that the average positive and negative surface electrostatic potentials of the cations and anions decrease with the size of the ion, as has been noted earlier. A model using computed statistical quantities has allowed us to put the melting points of both ionic solids and liquids together, covering a range from 993 °C to 11 °C.

1. Introduction to Electrostatic Potentials

The nuclei and electrons of an atom or molecule or ion create an electrostatic potential $V(\mathbf{r})$ at every point $\mathbf{r}$ in the surrounding space, given rigorously by the following equation:

$$V(\mathbf{r}) = \sum_A \frac{Z_A}{|\mathbf{R}_A - \mathbf{r}|} - \int \frac{\rho(\mathbf{r}')d\mathbf{r}'}{|\mathbf{r}' - \mathbf{r}|} \tag{1}$$

In Equation (1), Z_A is the charge on nucleus A, located at $\mathbf{R}_A$, and $\rho(\mathbf{r})$ is the system's electronic density. The sign of $V(\mathbf{r})$ in any region depends upon whether the positive contribution of the nuclei or the negative one of the electrons is dominant there.

Molecular electrostatic potentials were introduced as a tool in chemistry by Scrocco and Tomasi in the 1970s [1,2] and have been used extensively since then [3–5], and with considerable success, to interpret noncovalent interactions [6–9]; regions of positive and negative potential on one molecule will tend to interact favorably with, respectively, nucleophilic and electrophilic portions of another molecule. Of course, polarization, an intrinsic part of any Coulombic interaction [1,10], explains what are considered "counter-intuitive" interactions [11].

An important feature of the electrostatic potential is that it is a real physical property, an observable. It can be determined experimentally by diffraction methods [4,12,13] as well as computationally. The electrostatic potential should not be confused with partial atomic charges in molecules, which are arbitrarily defined (in many different ways) [11,14–19] because they are not physical observables. It should be noted, however, that some partial atomic charges have been designed to produce molecular dipole moments [18,19], which

are physical observables and which dominate the long-range part of a neutral molecule's electrostatic potential.

The electrostatic potential of a spherically symmetric neutral atom is positive everywhere (except, of course, at the actual position of the nucleus where it is undefined) and is monotonically decreasing as V(r) approaches infinity [3]; it is when atoms combine to form neutral molecules that negative regions of potential develop, often associated with lone pairs, π electrons and strained bonds [1–5], with associated global minima V_{min}. Pathak and Gadre showed that there are no global maxima [20], such that the minima must be linked by saddle points.

What is the situation with monoatomic ions and molecular ions? Spherically averaged monoatomic cations have positive potentials everywhere in space; the values of V(r) decrease monotonically as $r \to \infty$, as do their neutral counterparts [20,21]. Sen and Politzer proved in 1989 that the potential of monoatomic anions is positive close to the nucleus and then goes through a negative minimum, since $V(r) \to 0$ as $r \to \infty$ [22,23]. The positive monoatomic cations approach zero from the positive side, while the monoatomic anions approach zero from the negative side. The radial behavior of monoatomic ions has recently been revisited for both isotropic atoms and ions and the anisotropic halonium cations [24].

In using electrostatic potentials to analyze noncovalent interactions, V(**r**) is now generally computed on a molecular surface defined, following Bader et al., as an outer contour of the molecule's electronic density [25]. Defining the surface in this manner has the advantage that it reflects features specific to the particular molecule, such as lone pairs, π electrons and atomic anisotropy [6,9,26]. The 0.001 au contour is commonly chosen for this purpose, and the electrostatic potential on this contour is labeled $V_S(\mathbf{r})$. Its locally most positive and most negative values, of which there may be several, are designated by $V_{S,max}$ and $V_{S,min}$, respectively [26].

The useful information provided by a molecular surface electrostatic potential goes well beyond simply identifying positive and negative regions and utilizing the surface extrema. In the 1990s, Brinck et al. defined certain statistical quantities using the values of points on the surface electrostatic potential [27–29]; these have been found to be significant in quantifying important features of the surface electrostatic potentials of molecules [17,28–30].

The first such quantity defined was the average deviation of $V_S(\mathbf{r})$ [27]; it is a measure of the degree of internal charge separation that is present even in a molecule having a zero dipole moment, and is labeled Π [Equation (2)]:

$$\Pi = \frac{1}{n}\sum_{i=1}^{n}\left|V(\mathbf{r}_i) - \overline{V}_S\right| \tag{2}$$

where $\overline{V}_S$ is the average value of $V_S(\mathbf{r})$, while n is the number of points on the surface for which $V_S(\mathbf{r})$ is computed. This quantity has been shown to correlate with the Kamlet–Taft polarizability–polarity parameter and dielectric constants [27].

The next statistical quantities, the positive, negative and total variances of $V_S(\mathbf{r})$, were conceived to explain a trend seen in the solubilities of naphthalene and a series of substituted indoles in supercritical fluids [28]. These are defined in Equations (3)–(5) and reflect the ranges and variabilities of its positive and negative values, and of their sum.

$$\sigma_+^2 = \frac{1}{m}\sum_{i=1}^{m}\left[V^+(\mathbf{r}_i) - \overline{V}_S^+\right]^2 \tag{3}$$

$$\sigma_-^2 = \frac{1}{n}\sum_{j=1}^{n}\left[V^-(\mathbf{r}_j) - \overline{V}_S^-\right]^2 \tag{4}$$

$$\sigma_{tot}^2 = \sigma_+^2 + \sigma_-^2 \tag{5}$$

In Equations (3) and (4), the summations are over the surface points with positive and negative electrostatic potentials, respectively; $\overline{V}_S^+$ and $\overline{V}_S^-$ are the averages of the positive and negative values.

Finally, a balance parameter was defined to be a measure of the similarity between the positive and negative variances on the molecular surface [29], given by Equation (6).

$$\nu = \frac{\sigma_+^2 \, \sigma_-^2}{\left[\sigma_{tot}^2\right]^2} \tag{6}$$

Such a balance parameter was needed for obtaining correlations for properties that involve self-interaction, such as boiling points [29–31]. ν simply indicates how σ_+^2 and σ_-^2 compare. The more similar they are (whether large or small), the closer will ν be to its maximum possible value, 0.25, which corresponds to σ_+^2 and σ_-^2 being equal. The product of the total variance and the balance parameter, $\nu\sigma_{tot}^2$, has been found to be particularly effective for representing noncovalent molecular interactions involving self-interaction [17,30,31].

To give some perspective on these statistical quantities, Table 1 lists these quantities for water, ammonia, N_2 and a few small organic molecules, computed at the B3PW91/6-31G(d,p) level on 0.001 au iso-density surfaces. The molecules are listed in order of increasing size. It is noteworthy that water is the smallest molecule in Table 1 but has the largest Π, total variance, as well as ν and the product $\nu\sigma_{tot}^2$. This has been noted earlier [27,30,31]. The least balanced molecule in Table 1 is dimethyl ether, which helps to explain why its boiling point is similar to that of propane [27]. There are three molecules in Table 1 with zero dipole moments: methane, N_2 and acetylene. Their respective Π values of 3.0, 4.4 and 12.4 kcal/mol indicate that acetylene has the greatest internal charge separation of these three molecules, even though all three have zero dipole moments [27]. In addition, acetylene's value of $\nu\sigma_{tot}^2$ is indicative of it having greater interactive tendencies than do either methane or N_2.

Table 1. Computed values of molecular volumes (Vol), the average deviation of $V_S(\mathbf{r})$ (Π), positive, negative and total variances (σ_+^2, σ_-^2 and σ_{tot}^2), balance parameters ν and products $\nu\sigma_{tot}^2$ [a].

Molecule	Vol	Π	σ_+^2	σ_-^2	σ_{tot}^2	ν	$\nu\sigma_{tot}^2$
water	26.0	23.9	152.7	134.7	287.4	0.249	71.6
ammonia	33.6	17.9	38.8	185.4	224.2	0.143	32.1
N_2	35.5	4.4	4.9	7.2	12.1	0.241	2.9
methane	41.5	3.0	5.8	0.9	6.7	0.113	0.7
acetylene	48.1	12.4	77.3	27.7	105.0	0.194	20.4
methanol	50.9	13.5	89.7	139.3	229.0	0.238	54.5
dimethyl ether	75.7	8.7	6.2	118.3	124.5	0.047	5.8

[a] Units: Vol is in Å³; Π is in kcal/mol; σ_+^2, σ_-^2 and σ_{tot}^2 and $\nu\sigma_{tot}^2$ are in (kcal/mol)²; ν is dimensionless.

Most applications utilizing the statistical quantities defined in Equations (2)–(6) as well as surface areas and volumes have been applied to the physical properties of neutral molecules [17,26–32]. In contrast, our focus in this paper will be upon the surface electrostatic potentials of atomic and molecular cations and anions, highlighting previous work from the Politzer group [33–38] and by others [39–51]. Finally, we present data bridging concepts relevant to both ionic solids and liquids.

2. Methods

The structures and surface electrostatic potentials of all molecules and ions have been computed at the B3PW91/6-31G(d,p) level using G16 [52] and the WFA-SAS code [26]. This method/basis set combination has been shown to be reliable for our purposes [53].

3. Surface Electrostatic Potentials of Molecular Ions

The best way to introduce the electrostatic potentials of molecular ions is to compare them to those of neutral molecules. Take, for example, the series: NH_2NH_2, $NH_2NH_3^+$ and NH_2NH^-; their surface electrostatic potentials plotted on the 0.001 au contour of the electronic density are shown in Figure 1. Hydrazine has negative regions of $V_S(\mathbf{r})$ associated with the lone pairs on its nitrogens and positive regions associated with the hydrogens, shown in Figure 1a. The most positive regions on the surface of the hydrazinium cation are associated with the three hydrogens bonded to the nitrogen at the left in Figure 1b; the least positive region in blue is associated with the nitrogen at the right. Finally, the most negative region on the surface of NH_2NH^- is at the top right of Figure 1c, with the least negative sites (in red) on the hydrogens to left.
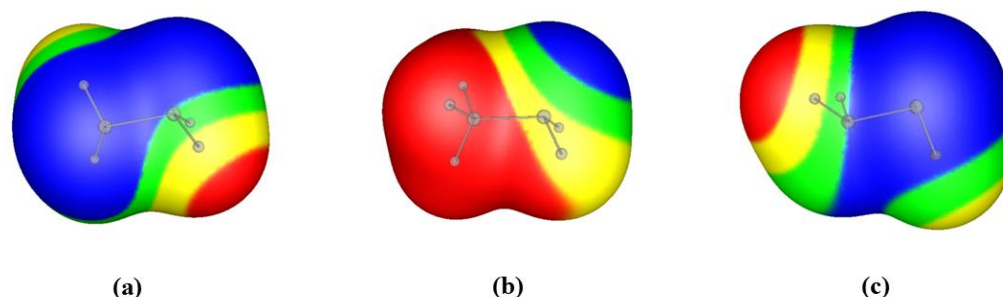

| (a) | (b) | (c) |

Figure 1. Computed electrostatic potentials on the 0.001 au iso-density contours of (**a**) hydrazine, (**b**) the hydrazinium cation, and (**c**) NH_2NH^-. The frameworks are shown in gray within the surfaces. The surface of (**a**) has both positive and negative values of $V_S(\mathbf{r})$; those of (**b**,**c**) are completely positive and negative, respectively. The color ranges, in kcal/mol, are therefore necessarily different for each. The color ranges for (**a**) are red, greater than 15; yellow, from 15 to 0; green, from 0 to −15; blue, more negative than −15. The color ranges for (**b**) are red, greater than 150; yellow, from 150 to 125; green, from 125 to 100; blue, less than 100. The color ranges for (**c**) are red, less negative than −110; yellow, from −110 to −130; green, from −130 to −150; blue, more negative than −150.

Neutral molecules such as those listed in Table 1 and hydrazine in Figure 1a typically have regions of both positive and negative electrostatic potential on their 0.001 au surfaces [1–9,26–32], while cations have only positive values of $V_S(\mathbf{r})$ and anions only negative values of $V_S(\mathbf{r})$ on these surfaces [33,35–39,41–51]. Monoatomic anions and molecular anions will have negative potentials when plotted on outer contours of the electronic density; however, at contours very close to the nuclei, the potentials will be positive, as they are there dominated by the first term in Equation (1) [22–24].

This is apparent from Figure 2, which shows $V(\mathbf{r})$ as a function of the distance r from the nucleus, labeled $V_{QC}(r)$ in the figure, for both Na^+ and F^-. The quantum chemically computed $V_{QC}(r)$ is compared with the electrostatic potential computed from a positive or negative unitary point charge, labeled $V_q(r)$ in the figure. $V_q(r)$ is obtained from Coulomb's law as $V_q(r) = q/r$. Note that for all values of r, $V_{QC}(r) > V_q(r)$, since a part of the electronic charge is located outside *r*. However, at larger distances this charge is very small and $V_{QC}(r)$ is nearly identical to $V_q(r)$, and the two curves are indistinguishable from each other. This is true already at the distance where $\rho(r) = 0.001$ au, which is the contour that we usually use for computing $V_S(\mathbf{r})$.

Sen and Politzer proved that the $V(r)$ of monoatomic singly negative spherically averaged ions must go through a minimum before approaching zero from the negative direction [22,23]. They also showed that these minima correspond to reasonable anionic radii for these ions and to lattice energies in a series of monoatomic cations (Li^+ to Fr^+) [22], and that the quantity of electronic charge encompassed within the radial V_{min} exactly equals the nuclear charge [22]. Ramasami and Murray recently showed that monoatomic spherically averaged ions with charges greater than −1 follow the same pattern [24]. As

expected, F^- also has a radial V_{min}, and, as shown in Figure 2, it appears at a much shorter distance than the 0.001 density contour.
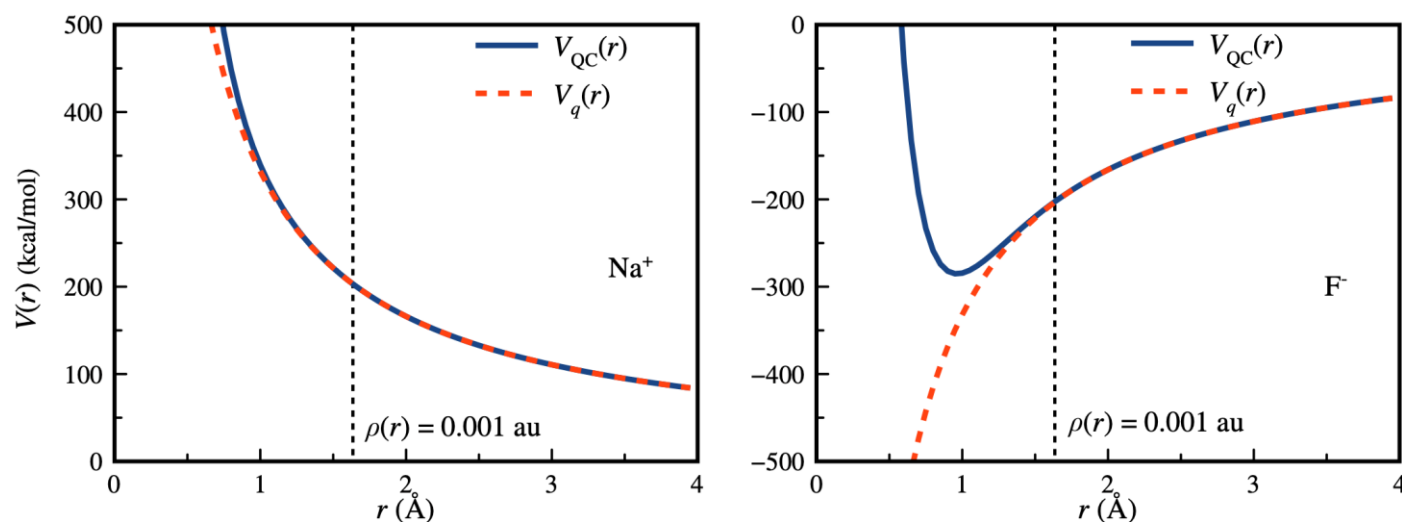

Figure 2. The quantum chemically computed electrostatic potential ($V_{QC}(r)$) compared with the electrostatic potential of a point charge ($V_q(r)$) as functions of the distance (r) from the nucleus for the ions Na^+ and F^-. The distance of the iso-density contour ($\rho(r) = 0.001$ au) that is used to compute $V_S(r)$ is marked in both plots.

Our first venture into looking at the statistical quantities of charged species larger than monoatomic ions was looking at lattice energies of a series of 17 anions, ranging in size from F^- to $SiF_6{}^{-2}$ and including both inorganic and organic ions with charges primarily of -1 but a few with charges of -2 [33]. What we found is that for NH_4^+, Na^+ and K^+ salts, there were good correlations between the charge Q of the anion, the $V_{S,min}$ on the surface of the anion and the product of the $V_{S,min}$ and the surface area of the anion [33].

Zwitterions are neutral but locally have stronger positive and negative regions of electrostatic potential in the vicinities of their positive- and negative-charged regions than do their nonionic counterparts [34]. This was explored for glycine, histidine and tetracycline. The average deviations of the surface electrostatic potentials of the zwitterions, the Π values, were in each instance greater for the zwitterionic forms than for the nonionic forms [34].

Moving on to molecular cations, a study was planned and carried out to assess the stability of gas phase carbocations [35]. What was found is that the stabilities of the carbocations generally follow the decrease of their $V_{S,max}$ values. This follows intuitively, as the $+1$ charge is more delocalized as the size of carbocation increases, and the $V_{S,max}$ value accordingly decreases [35].

In 2009, Politzer et al. published a paper entitled "An electrostatic interaction correction for improved crystal density prediction" [54]. The objective of this paper was to improve crystal density predictions for energetic molecules. In this paper, the authors added an electrostatic correction term to the already widely used term M/V_m [55,56], where M is the molecular mass and V_m is the volume of the 0.001 au iso-density surface envelope encompassing the molecule. Both statistical quantities Π and $\nu\sigma_{tot}^2$ were tested and yielded improved predictions [54]. A reviewer for this paper wondered if this could somehow be extended to energetic ionic salts.

This led to exploratory computational work involving energetic ionic salts; it seemed reasonable and necessary to find a correction term for the cation and the anion in each salt.

For a dataset of 25 energetic ionic salts, we found the following equation to be an effective option [36]:

$$\text{density} = \alpha \frac{M}{V_m} + \beta \left(\frac{\overline{V_S^+}}{A_S^+} \right) + \gamma \left(\frac{\overline{V_S^-}}{A_S^-} \right) + \delta \tag{7}$$

where $\overline{V_S^+}$ and $\overline{V_S^-}$ are the average values of the potential on the surfaces of the cations and anions, respectively, and A_S^+ and A_S^- are the surface areas of the positive cations and negative anions. M is the molecular mass of the salt, and V_m is the sum of the 0.001 au volumes of the cation (s) and anion (s) for each salt. This improvement over M/V_m alone could be further explored, as has been pointed out [36]. Statistical quantities derived from the surface electrostatic potential together with other descriptors have also been used to develop machine learning models for prediction of solvation and partition properties of ionic liquids [57,58].

Finally, some perspectives on the sensitivities of ionic energetic materials were addressed by Politzer et al. [37,38] after some interest toward this endeavor was expressed. This is a challenge that continues to this day. One of the findings found computationally is that the impact sensitivities for a series of ammonium salts showed a tendency to decrease as the absolute value of the differences of the most negative surface potentials, the $V_{S,min}$, and the least negative surface potentials, the $V_{S,max}$, of the anions increased [38]. Further investigations of this complex phenomenon are warranted.

4. Statistical Quantities of Some Cations and Anions in Ionic Salts and Liquids

Table 2 lists surface areas, volumes and some statistical quantities defined in terms of the electrostatic potential on the surfaces of a number of cations and anions that can be components of ionic salts and liquids. Ionic salts are solids at room temperature, while ionic liquids are generally defined as having melting points below 100 °C [59–61], with room-temperature ionic liquids having melting points below 25 °C. The ethylammonium, trimethylammonium, 1-ethyl-3-methylimidazolium and 1-butyl-3-methylimidazolium cations are given the common abbreviations EA$^+$, TMA$^+$, EMIM$^+$ and BMIM$^+$ in Table 2. All of the ions in Table 2 have a charge of ± 1.

Table 2. Computed surface quantities for a number of cations and anions.

Cation or Anion	Surface Area (Å^2)	Volume (Å^3)	$\overline{V_S^+}$ or $\overline{V_S^-}$ (kcal/mol)	Π (kcal/mol)	σ_+^2 or σ_-^2 (kcal/mol)^2	$V_{S,max}$ (kcal/mol)	$V_{S,min}$ (kcal/mol)
Na$^+$	22.3	9.88	250.0	0	0	250.0	250.0
K$^+$	38.4	22.35	191.1	0	0	191.1	191.1
NH$_4^+$	47.5	30.13	171.8	3.6	17.7	180.6	164.9
EA$^+$	95.2	77.13	124.5	23.1	655	164.0	87.8
TMA$^+$	131.1	125.9	107.6	10.7	176	146.7	90.3
EMIM$^+$	163.8	153.4	96.6	8.6	121	122.8	72.2
BMIM$^+$	208.1	201.5	86.1	15.3	330	120.7	49.1
F$^-$	33.6	18.31	-202.6	0	0	-202.6	-202.6
Cl$^-$	60.9	44.72	-149.1	0	0	-149.1	-149.1
Br$^-$	66.9	51.44	-142.4	0	0	-142.4	-142.4
NO$_3^-$	77.6	58.25	-134.1	4.8	37.0	-117.9	-150.6
BF$_4^-$	82.4	62.47	-131.5	4.2	23.9	-121.6	-142.6
PF$_6^-$	104.6	87.69	-118.0	4.3	24.5	-108.5	-125.5
MeSO$_4^-$	119.6	106.05	-109.4	24.3	754	-52.1	-139.0

To provide some perspective and to allow the reader to visualize the potentials, Figures 3 and 4 show the $V_S(\mathbf{r})$ of the cations EA$^+$ and BMIM$^+$ and the anions BF$_4^-$ and PF$_6^-$, respectively. The surfaces of the cations shown in Figure 3 are totally positive, showing variation in their surface electrostatic potentials, as has been noted recently for EMIM+ [49]. The larger color range cutoffs for EA$^+$ compared to those of BMIM$^+$ are consistent with their respective average positive surface potentials $\overline{V}_S^+$ listed in Table 2, 124.5 vs. 86.1 kcal/mol, and their sizes. The most positive regions of EA$^+$ are associated with the hydrogens bonded to the nitrogen on the left in Figure 3a and can be compared to those of the hydrazinium cation in Figure 1b. The most positive region in Figure 3b is to the bottom left in the region, between the C-2 hydrogen and the closest methyl hydrogen of the C-3 methyl group, where the positive regions overlap on the surface.
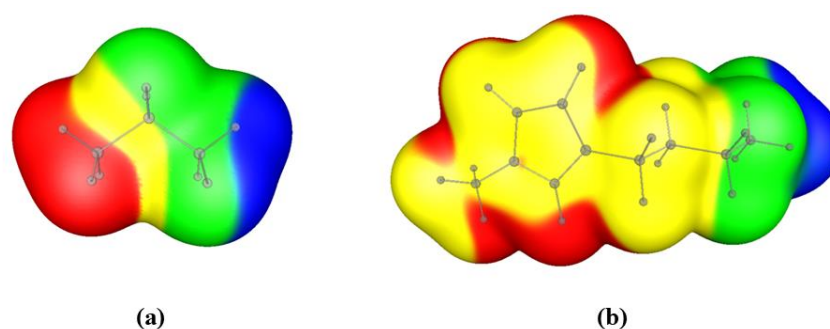

(a)   (b)

Figure 3. Computed electrostatic potentials on the 0.001 au iso-density contours of (**a**) EA$^+$ and (**b**) [BMIM]$^+$. The frameworks are shown in gray within the surfaces. The color ranges, in kcal/mol, are for (**a**) red, greater than 150; yellow, from 150 to 125; green, from 125 to 100; blue, less than 100. The color ranges for (**b**) are red, greater than 100; yellow, from 100 to 80; green, from 80 to 60; blue, less than 60.
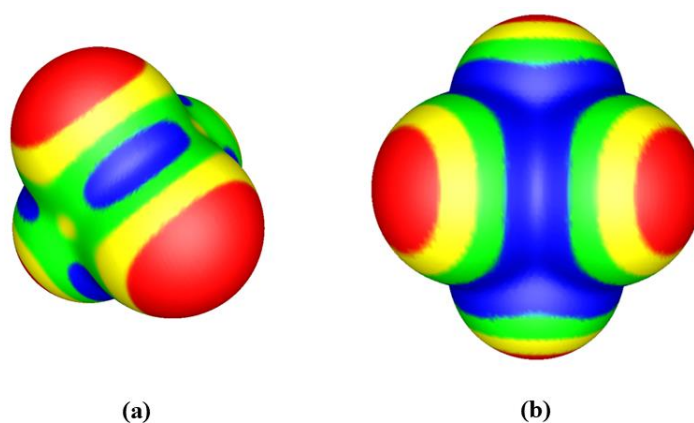

(a)   (b)

Figure 4. Computed electrostatic potentials on the 0.001 au iso-density contours of (**a**) BF$_4^-$ and (**b**) PF$_6^-$. The color ranges, in kcal/mol, are for (**a**) red, less negative than -129; yellow, from -129 to -133; green, from -133 to -137; blue, more negative than -137. The color ranges for (**b**) are red, less negative than -113; yellow, from -113 to -117; green, from -117 to -121; blue, more negative than -12.

What is interesting to observe in Figure 4 is the fact that the color range cutoffs for both anions cover only a narrow range, compared to those of the cations shown in Figure 3. Those of BF$_4^-$ are only slightly more negative than those of PF$_6^-$, and are consistent with their sizes, their $\overline{V}_S^-$ values and the ranges of their negative potentials (Table 2).

The cations are listed first in Table 2, from smallest to largest, as indicated by their surface areas and volumes. These are followed by the anions. Note that the average surface potentials $\overline{V}_S^+$ and $\overline{V}_S^-$ for the cations and anions, respectively, decrease in magnitude in the

same order that size increases. This has been observed in earlier studies [33,35–38] and can be attributed to the overall charge of each ion, either +1 or −1, being delocalized over a larger space as the size of the ion increases. For each monoatomic cation and anion, the $V_{S,max}$ and $V_{S,min}$ values are the same, as their potentials are isotropic [20–24], explaining why their Π and σ_+^2 or σ_-^2 values are zero. This is not the case for the molecular cations and anions, which show variation in their electrostatic potentials, as shown by their Π, σ_+^2 or σ_-^2 values as well as their $V_{S,max}$ and $V_{S,min}$ values.

Do the data in Table 2 reflect features of the cations and anions that relate to the melting points of some ionic salts and ionic liquids? To explore this possibility, in Table 3 are listed some melting points [62,63] for seventeen ionic salts and liquids. Note that the ionic salts have melting points often an order of magnitude greater, or more, than those of the ionic liquids. It can be seen in Table 2 that Na^+ and K^+ are the two smallest cations listed and that they have the two largest average values ($\overline{V}_S^+$), while the halide ions are the three smallest anions and have the three most negative $\overline{V}_S^-$, with the fluoride ion's value being significantly more negative than those of the chloride and bromide ions. Another observation is that the surface areas and volumes of the cations cover a wider range of values than those of the anions.

Table 3. List of experimentally determined and predicted melting points (mps) for some ionic salts and liquids.

Ionic Salt or Liquid	Mp (°C) [a] [Exp]	Mp (°C) [Pred]
NaF	993	984
KF	858	891
NaCl	800	790
KCl	770	743
NaBr	747	766
KBr	730	724
$NH_4^+Cl^-$	338	266
$NH_4^+Br^-$	235	249
$NH_4^+NO_3^-$	169.6	228
$[BMIM]^+Br^-$	78.2	56
$[EMIM]^+Br^-$	76.8	67
$[EMIM]^+PF_6^-$	60.1	33
$[BMIM]^+Cl^-$	67.85	65
$[BMIM]^+NO_3^-$	36.01	46
$[EMIM]^+BF_4^-$	14	52
$[EA]^+NO_3^-$	12	11
$[BMIM]^+PF_6^-$	11.4	26

[a] Taken from references [58,59].

With some insight from earlier work with ionic systems [31,33–36], the following multivariable relationship was found for the seventeen ionic salts and liquids in Table 3 using the NCSS software [64]:

$$\text{melting point} = 182.0\,\overline{V}_S^+ - 0.01445\left(\overline{V}_S^+\,\overline{V}_S^-\right) + 2.491\left(A_S^+\overline{V}_S^+\right) - 1174\left(\frac{\overline{V}_S^+}{A_S^+}\right) + \tag{8}$$
$$-72.83\left(\text{Vol}^+\right) - 45267$$

where $\overline{V}_S^+$ and $\overline{V}_S^-$ are the average values of the potential on the surfaces of the cations and anions, respectively, and A_S^+ and Vol^+ are the surface areas and volumes of the positive

cations. Note that the second term in Equation (8) is a cross-term, $(\overline{V_S^+}\,\overline{V_S^-})$, fitting in with the Coulombic nature of ionic interactions. The first three terms in Equation (8) lead to an increase in the value of the melting point, with the fourth and fifth terms serving likely as correction terms. The R value for the correlation is 0.997 and the F-ratio is 328, showing improvement over any three- or four-variable correlations. Each term in Equation (8) has a *p*-value of 0.000, indicating the validity of each variable.

A plot of predicted vs. experimentally determined melting points is shown as Figure 5. As can be clearly seen the points for the ionic salts are at the top right of the plot, while those of the ionic liquids are at the bottom left, with the ammonium salts in between.
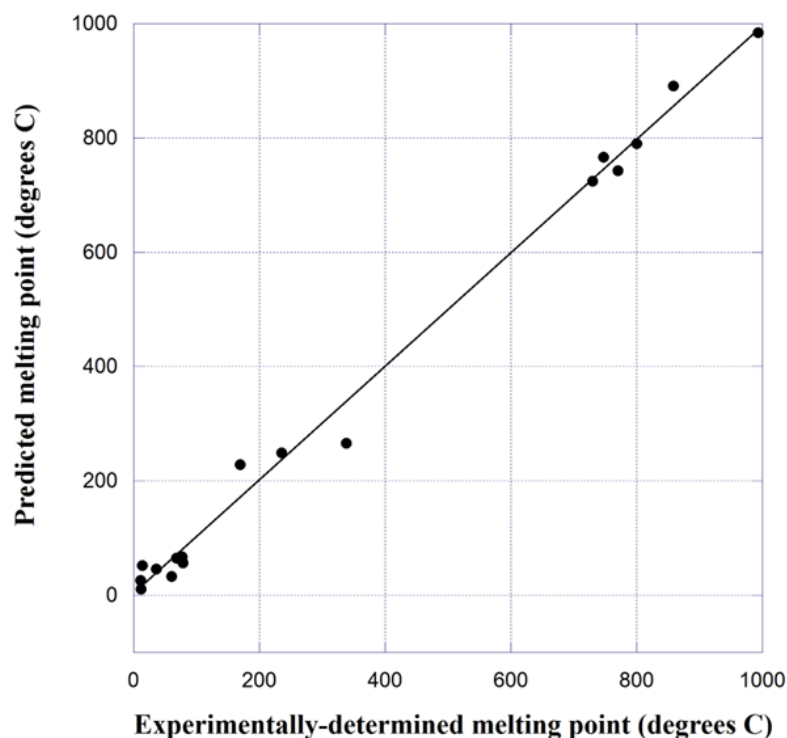
Figure 5. Plot of predicted melting points using Equation (8) vs. experimentally determined melting points for the seventeen ionic systems in Table 3. R = 0.997.

In the correlation shown in Equation (8) and in the corresponding plot in Figure 5, the variables relating to the cations emerge as appearing more relevant than those for the anions. In fact, the only inclusion of the average negative surface electrostatic potential $\overline{V_S^-}$ is in the cross-term $(\overline{V_S^+}\,\overline{V_S^-})$. This suggests that perhaps other contours of the electronic density might be better for characterizing the anions. As was shown recently, the radial V_{min} for sphericallysymmetric monoatomic anions is within their 0.001 au iso-density surfaces [22]. Another possibility is that the characteristics of the cations are simply more important.

5. Concluding Remarks

In this paper we have reviewed statistical quantities defined in terms of the surface electrostatic potential; these were originally defined to quantify the wealth of information beyond surface extrema that surface electrostatic potential plots provide. The original applications of these quantities were primarily for neutral molecules.

This study surveys earlier uses of the statistical quantities for ionic solids and is to be viewed as a starting point for future explorations in the growing field of ionic liquids. The properties of ionic liquids are complex; it may be that further studies involving surface electrostatic potential statistical quantities, as well as surface areas and volumes, will prove fruitful in this area.

References

1. Scrocco, E.; Tomasi, J. The Electrostatic Molecular Potential as a Tool for the Interpretation of Molecular Properties. In *New Concepts II. Topics in Current Chemistry*; Springer: Berlin, Germany, 1973; Volume 42, pp. 95–170.
2. Scrocco, E.; Tomasi, J. Electronic Molecular Structure, Reactivity and Intermolecular Forces: An Euristic Interpretation by Means of Electrostatic Molecular Potentials. *Adv. Quant. Chem.* **1978**, *11*, 115–193.
3. Politzer, P.; Daiker, K.C. Models for Chemical Reactivity. In *The Force Concept in Chemistry*; Deb, B.M., Ed.; Van Nostrand Reinhold: New York, NY, USA, 1981; Chapter 6, pp. 294–387.
4. Politzer, P.; Truhlar, D.G. (Eds.) *Chemical Applications of Atomic and Molecular Electrostatic Potentials*; Plenum: New York, NY, USA, 1981.
5. Politzer, P.; Murray, J.S. Molecular Electrostatic Potentials and Chemical Reactivity. In *Reviews in Computational Chemistry*; Lipkowitz, K.B., Boyd, D.B., Eds.; VCH Publishers: New York, NY, USA, 1991; Volume 2, pp. 273–312.
6. Brinck, T. The Use of the Electrostatic Potential for Analysis and Prediction of Intermolecular Interactions. In *Theoretical Organic Chemistry*; Parkanyi, C., Ed.; Elsevier: Amsterdam, The Netherlands, 1998; pp. 51–93.
7. Hunter, C.A. Quantifying intermolecular interactions: Guidelines for the molecular recognition toolbox. *Angew. Chem. Int. Ed.* **2004**, *43*, 5310–5324. [CrossRef] [PubMed]
8. Aakeröy, C.B.; Wijethunga, T.K.; Desper, J. Molecular electrostatic potential dependent selectivity of hydrogen bonding. *New J. Chem.* **2015**, *39*, 822–828. [CrossRef]
9. Murray, J.S.; Politzer, P. Molecular electrostatic potentials and noncovalent interactions. *WIREs Comput. Mol. Sci.* **2017**, *7*, e1326. [CrossRef]
10. Francl, M.M. Polarization corrections to electrostatic potentials. *J. Phys. Chem.* **1985**, *89*, 428–433. [CrossRef]
11. Clark, T.; Murray, J.S.; Politzer, P. A perspective on quantum mechanics and chemical concepts in describing noncovalent interactions. *Phys. Chem. Chem. Phys.* **2018**, *20*, 30076–30082. [CrossRef]
12. Stewart, R.F. On the mapping of electrostatic properties from Bragg diffraction data. *Chem. Phys. Lett.* **1979**, *65*, 335–342. [CrossRef]
13. Klein, C.L.; Stevens, E.D. Experimental measurements of electron density distributions and electrostatic potentials. In *Structure and Reactivity*; Liebman, J.F., Greenberg, A., Eds.; VCH Publishers: New York, NY, USA, 1988; pp. 25–64.
14. Bachrach, S.M. Population analysis and electron densities from quantum mechanics. In *Reviews in Computational Chemistry*; Lipkowitz, K.B., Boyd, D.B., Eds.; VCH Publishers: New York, NY, USA, 1994; Volume 5, pp. 171–227.
15. Naray-Szabo, G.; Ferenczy, G. Molecular electrostatics. *Chem. Rev.* **1995**, *95*, 829–847. [CrossRef]
16. Price, S.L. Applications of realistic electrostatic modelling to molecules in complexes, solids and proteins. *J. Chem. Soc. Faraday Trans.* **1996**, *92*, 2997–3008. [CrossRef]
17. Murray, J.S.; Politzer, P. The electrostatic potential: An overview. *WIREs Comput. Mol. Sci.* **2011**, *1*, 153–163. [CrossRef]
18. Marenich, A.V.; Jerome, S.V.; Cramer, C.J.; Truhlar, D.G. Charge model 5: An extension of the Hirshfeld population analysis for the accurate description of molecular interactions in ground and excited states in the vapor and in condensed phases. *J. Chem. Theory Comput.* **2012**, *8*, 527–541. [CrossRef] [PubMed]
19. Liu, S.; Luan, B. Benchmarking various types of partial atomic charges for classical all-atom simulations of metal-organic frameworks. *Nanoscale* **2022**, *14*, 9466–9473. [CrossRef] [PubMed]
20. Pathak, R.K.; Gadre, S.R. Maximal and minimal characteristics of molecular electrostatic potentials. *J. Chem. Phys.* **1990**, *93*, 1770–1773. [CrossRef]
21. Weinstein, H.; Politzer, P.; Srebrenik, S. A misconception concerning the electronic density distribution of an atom. *Theor. Chim. Acta* **1975**, *38*, 159–163. [CrossRef]
22. Sen, K.D.; Politzer, P. Characteristic features of the electrostatic potentials of singly-negative monoatomic ions. *J. Chem. Phys.* **1989**, *90*, 4370–4372. [CrossRef]

23. Sen, K.D.; Politzer, P. Approximate radii for singly-negative ions of 3d, 4d and 5d metal ions. *J. Chem. Phys.* **1989**, *91*, 5123–5124. [CrossRef]

24. Ramasami, P.; Murray, J.S. Radial behavior of atoms and ions revisited: Isotropy and anisotropy. *ChemPhysChem* **2024**, *25*, e202400450. [CrossRef]

25. Bader, R.F.W.; Carroll, M.T.; Cheeseman, J.R.; Chang, C. Properties of atoms in molecules. Atomic volumes. *J. Am. Chem. Soc.* **1987**, *109*, 7968–7979. [CrossRef]

26. Bulat, F.A.; Toro-Labbé, A.; Brinck, T.; Murray, J.S.; Politzer, P. Quantitative analysis of molecular surfaces: Areas, volumes, electrostatic potentials and average local ionization energies. *J. Mol. Model.* **2010**, *16*, 1679–1691. [CrossRef]

27. Brinck, T.; Murray, J.S.; Politzer, P. Quantitative determination of the total local polarity (charge separation) in molecules. *Mol. Phys.* **1992**, *76*, 609–616. [CrossRef]

28. Politzer, P.; Lane, P.; Murray, J.S.; Brinck, T. Investigation of relationships between solute molecule surface electrostatic potentials and solubilities in supercritical fluids. *J. Phys. Chem.* **1992**, *96*, 7938–7943. [CrossRef]

29. Murray, J.S.; Lane, P.; Brinck, T.; Paulsen, K.; Grice, M.E.; Politzer, P. Relationships of critical constants and boiling points to computed molecular surface properties. *J. Phys. Chem.* **1993**, *97*, 9369–9373. [CrossRef]

30. Murray, J.S.; Brinck, T.; Lane, P.; Paulsen, K.; Politzer, P. Statistically-based interaction indices derived from molecular surface electrostatic potentials; A general interaction properties function (GIPF). *J. Mol. Struct. (Theochem)* **1994**, *307*, 55–64. [CrossRef]

31. Politzer, P.; Murray, J.S. Computational prediction of condensed phase properties from statistical characterization of molecular surface electrostatic potentials. *Fluid Phase Equil.* **2001**, *185*, 129–137. [CrossRef]

32. Murray, J.S.; Seybold, P.G.; Battino, R.; Politzer, P. A general model for the solubilities of gases in liquids. *J. Mol. Model.* **2020**, *26*, 244. [CrossRef]

33. Politzer, P.; Murray, J.S. Relationships between lattice energies and surface electrostatic potentials and areas of anions. *J. Phys. Chem. A* **1998**, *102*, 1018–1020. [CrossRef]

34. Murray, J.S.; Peralta-Inga, Z.; Politzer, P. Computed molecular surface electrostatic potentials of the nonionic and zwitterionic forms of glycine, histidine and tetracycline. *Int. J. Quant. Chem.* **2000**, *80*, 1216–1223. [CrossRef]

35. Robbins, A.M.; Jin, P.; Brinck, T.; Murray, J.S.; Politzer, P. The electrostatic potential as a measure of gas phase carbocation stability. *Int. J. Quant. Chem.* **2006**, *106*, 2904–2909. [CrossRef]

36. Politzer, P.; Martinez, J.; Murray, J.S.; Concha, M.C. An electrostatic correction for improved crystal density predictions of energetic ionic compounds. *Mol. Phys.* **2010**, *108*, 1391–1396. [CrossRef]

37. Politzer, P.; Lane, P.; Murray, J.S. Electrostatic potentials, intralattice attractive forces and crystal densities of nitrogen-rich C,H,N,O salts. *Crystals* **2016**, *6*, 7. [CrossRef]

38. Politzer, P.; Lane, P.; Murray, J.S. Sensitivities of ionic explosives. *Mol. Phys.* **2017**, *115*, 497–509. [CrossRef]

39. Cavallo, G.; Murray, J.S.; Politzer, P.; Ursini, M.; Resnati, G. Halogen bonding in hypervalent iodine and bromine derivatives: Halonium salts. *Int. Union Crystallogr. J.* **2017**, *4*, 411–419. [CrossRef] [PubMed]

40. Stenlid, J.H.; Brinck, T. Extending the σ-hole concept to metals: An electrostatic interpretation of the effects of nanostructure in gold and platinum catalysis. *J. Am. Chem. Soc.* **2017**, *139*, 11012–11015. [CrossRef] [PubMed]

41. Lim, J.Y.C.; Beer, P.D. Sigma-hole interactions in anion recognition. *Chem* **2018**, *4*, 731–783. [CrossRef]

42. Konidaris, K.F.; Pilati, T.; Terraneo, G.; Politzer, P.; Murray, J.S.; Scilabra, P.; Resnati, G. Cyanine dyes: Synergistic action of hydrogen, halogen and chalcogen bonds allows $I_4{}^{2-}$ anions in crystals. *New J. Chem.* **2018**, *42*, 10463–10466. [CrossRef]

43. Scilabra, P.; Murray, J.S.; Terraneo, G.; Resnati, G. Chalcogen bonds in crystals of bis(*o*-anilinium)diselenide salts. *Cryst. Growth Des.* **2019**, *19*, 1149–1154. [CrossRef]

44. Williams, I.M.; Qasim, L.N.; Tran, L.; Scott, A.; Riley, K.; Dutta, S. C-D vibration at C2 position of imidazolium cation as a probe of the ionic liquid microenvironment. *J. Phys. Chem. A* **2019**, *123*, 6342–6349. [CrossRef]

45. Daolio, A.; Pizzi, A.; Calabrese, M.; Terraneo, G.; Bordignon, S.; Frontera, A.; Resnati, G. Anion—Anion coinage bonds: The case of tetrachloridoaurate. *Angew. Chem. Int. Ed.* **2021**, *60*, 14385–14389. [CrossRef]

46. Tran, L.; Rush, K.; Marzette, J.; Edmonds-Andrews, G.; Bennett, T.; Abdulahad, A.; Riley, K.E.; Dutta, S. Striking temperature-dependent molecular reorganization at the C-2 position of [EMIM][BF$_4$]. *Chem. Phys. Lett.* **2021**, *783*, 138956. [CrossRef]

47. Konidaris, K.; Daolio, A.; Pizzi, A.; Scilabra, P.; Terraneo, G.; Quici, A.; Murray, J.S.; Politzer, P.; Resnati, G. Thiazolium salts as chalcogen bond donors. *Cryst. Growth Des.* **2022**, *22*, 4987–4995. [CrossRef]

48. Calabrese, M.; Pizzi, A.; Beccaria, R.; Frontera, A.; Resnati, G. Halogen bonding assembles anion—Anion architectures in non-centrosymmetric iodate and bromate crystals. *ChemPhysChem* **2023**, *24*, e202300298. [CrossRef] [PubMed]

49. Rush, K.; Islam, M.M.; Nawagamuwage, S.U.; Marzette, J.; Browne, O.; Foy, K.; Reyes, K.; Hoang, M.; Nguyen, C.; Walker, A.; et al. Hydrogen-bonded complexes in binary mixture of imidazolium-based ionic liquids with organic solvents. *J. Phys. Chem. B* **2023**, *127*, 8916–8925. [CrossRef] [PubMed]

50. Wieske, L.H.E.; Erdélyi, M. Halogen Bonds of Halogen(I) Ions—Where Are We and Where to Go? *J. Am. Chem. Soc.* **2024**, *146*, 3–18. [CrossRef] [PubMed]

51. Puttreddy, R.; Kuma, P.; Rissanen, K. Pyridine iodine (I) cations: Kinetic trapping as a sulfonate complexes. *Chem. Eur. J.* **2024**, *30*, e202304178. [CrossRef] [PubMed]

52. Frisch, M.J.; Trucks, G.W.; Schlegel, H.B.; Scuseria, G.E.; Robb, M.A.; Cheeseman, J.R.; Scalmani, G.; Barone, V.; Petersson, G.A.; Nakatsuji, H.; et al. *Gaussian 16, Revision C.01*; Gaussian, Inc.: Wallingford, CT, USA, 2016.

53. Riley, K.E.; Tran, K.; Lane, P.; Murray, J.S.; Politzer, P. Comparative analysis of electrostatic potential maxima and minima on molecular surfaces, as determined by three methods and a variety of basis sets. *J. Comput. Sci.* **2016**, *17*, 273–284. [CrossRef]
54. Politzer, P.; Martinez, J.; Murray, J.S.; Concha, M.C.; Toro-Labbé, A. An electrostatic interaction correction for improved crystal density prediction. *Mol. Phys.* **2009**, *107*, 2095–2101. [CrossRef]
55. Qiu, L.; Xiao, H.; Gong, X.; Ju, X.; Zhu, W. Crystal density predictions for nitramines based on quantum chemistry. *J. Hazard. Mater.* **2007**, *141*, 280–288. [CrossRef]
56. Rice, B.M.; Hare, J.J.; Byrd, E.F.C. Accurate predictions of crystal densities using quantum mechanical molecular volumes. *J. Phys. Chem. A* **2007**, *111*, 10874–10879. [CrossRef]
57. Chang, J.-X.; Zou, J.-W.; Lou, C.-Y.; Ye, J.-X.; Feng, R.; Li, Z.-Y.; Hu, G.-X. Gas-to-ionic liquid partition: QSPR modeling and mechanistic interpretation. *Mol. Inf.* **2023**, *42*, 2200223. [CrossRef]
58. Zhang, Z.-Y.; Wang, X.; He, Q.; Sun, Z. Chemical accuracy prediction of molecular solvation and partition in ionic liquids with educated estimators. *J. Mol. Liq.* **2023**, *391*, 123202. [CrossRef]
59. Hallett, J.P.; Welton, T. Room-temperature ionic liquids: Solvents for synthesis and catalysis. 2. *Chem. Rev.* **2011**, *111*, 3508–3576. [CrossRef] [PubMed]
60. Hayes, R.; Warr, G.G.; Atkin, R. Structure and nanostructure in ionic liquids. *Chem. Rev.* **2015**, *115*, 6357–6426. [PubMed]
61. Lei, Z.; Chen, B.; Koo, Y.-M.; MacFarlane, D.R. Introduction: Ionic liquids. *Chem. Rev.* **2017**, *117*, 6633–6635. [CrossRef] [PubMed]
62. Rumble, J.R., Jr.; Bruno, T.J.; Doa, M.J. (Eds.) *Handbook of Chemistry and Physics*, 101st ed.; CRC Press: Boca Raton, FL, USA, 2021.
63. Available online: https://en.wikipedia.org/wiki (accessed on 23 October 2024).
64. *NCSS 2024 Statistical Software*; NCSS, LLC: Kaysville, UT, USA, 2024. Available online: https://www.ncss.com/software/ncss (accessed on 23 October 2024).